



Palladium(II) based imines; synthesis, characterization, X-Ray structural analysis; DFT and catalytic hydrogenation study

Mohamed M. Ibrahim^a, Ahmed M. Fathy^b, Sami A. Al-Harbi^c, Shehab A. Sallam^d,
Salih S. Al-Juaid^e, Abd El-Motaleb M. Ramadan^{f,*}

^a Chemistry Department, Faculty of Science, Taif University, Taif, P. O. Box 11099, Taif 21944, Saudi Arabia

^b Chemistry Department, Faculty of Science, Zagazig University, Zagazig Egypt

^c Chemistry Department of, University College in Al-Jamoum, Umm Al-Qura University, Makkah, Saudi Arabia

^d Department of Chemistry, Faculty of Science, Suez Canal University, Ismailia, Egypt

^e Department of Chemistry, Faculty of Science, King Abdul-Aziz University, Jeddah, Saudi Arabia

^f Chemistry Department, Faculty of Science, Kafr El-Sheikh University, Kafr El-Sheikh Egypt

ARTICLE INFO

Article history:

Received 25 January 2021

Revised 21 February 2021

Accepted 25 February 2021

Available online 1 March 2021

Keywords:

Synthesis

Characterization

Schiff bases

Palladium(II) complexes

DFT study

Hydrogenation

ABSTRACT

Based on the bridge alkyl chain length between the two azomethine linkages of the bis ortho naphtholimine ligands, two synthetic techniques were used to prepare a novel series of palladium(II) complexes. The molecular formulae of the isolated metal chelates were assigned based on thermal analysis (TGA and DTA) and analytical data. In addition comprehensive spectroscopic studies such as UV-Vis, IR, PXRD and X-ray single crystal have completed the structural formulations of the newly synthesized palladium(II) complexes in question. The best description of the overall molecular geometry of the palladium(II) center is the square planar as expected for the d^8 center of palladium(II). DFT calculations were performed to correlate the structural properties of the present palladium(II) complexes with their catalytic activity towards the hydrogenation of cyclohexene. In addition, the optimized geometrical parameters deduced from the X-ray measurements for structural analysis are compared with the corresponding ones obtained by DFT calculations. Regarding complex **3**, DFT calculations were carried out to decide the most appropriate molecular structure. The current square planar diimine palladium(II) complexes have been evaluated for the catalytic hydrogenation of mono olefin cyclohexene. The catalytic activity was studied in relation to the effect of catalyst structure, catalysis type, nature and amount of the solvents and co-solvents. The results obtained indicated that these complexes are pre-catalysts that efficiently catalyze hydrogenation of cyclohexene by H_2 at mild conditions.

© 2021 Elsevier B.V. All rights reserved.

1. Introduction

Among the most frequently used reactions in the synthesis of biological materials, pharmaceuticals, dyestuffs, plastics, petrochemicals, fine chemicals and commodities is the catalytic hydrogenation of the unsaturated hydrocarbons by transition metal complexes [1]. Therefore renewed interest in developing catalysts for hydrogenation of alkenes has been emerged over the current decade [2]. In this regard, catalytic hydrogenation of an inactive olefin is one of the most promising methods for developing a robust synthetic method with low economic and environmental impacts. Previous reports have shown that higher activity, sulfur resistance and working under milder reaction conditions are the ad-

vantages of metal complex over the metal itself [3]. As a result, a broad range of metal complexes derived from electron rich divalent metal ions of group 10 metals now are known to function as hydrogenation catalysts under moderate conditions [4]. To date, palladium(II)-based catalysts have received great interest in the hydrogenation of alkenes as a result of their stability, highly catalytic and selective activities [5].

Metal complexes of Schiff base have occupied a central role in the development of coordination chemistry. This situation is evidenced by the sheer number of publications that showered from pure physical chemistry to modern physical chemistry and studies related to the biochemistry of these metal complexes. Among of these Schiff base metal complexes deserve mention as hydrogenation catalysts, the palladium(II) with square-planar chelating Schiff base ligand (salen), [N,N-ethylene bis-(salicyldeneiminato)Pd(II)] which has been suggested as model for the natural hydrogenating system (hydrogenases) due to the mechanistic similarity [6].

* Corresponding author.

E-mail address: Ramadanss@hotmail.com (A.E.M. Ramadan).

In the catalytic hydrogenation reactions of alkenes, by transition metal complexes, the substantial processes of breaking and making bonds, such as oxidative addition and reductive elimination, often depend on the flexibility of the central metal ion that is adjusted by the coordinated ligand. Thus ligand design and coordination environment around the metal ion are key to the catalytic performance of metal complexes that catalyze the hydrogenation reactions of alkenes. In this regard, diimine tetradentate based metal complexes have been shown to be more operative in catalysis of the alkenes hydrogenation [6,7] Palladium(II) complexes containing quadridentate diimine ligands derived from salicylaldehyde have demonstrated their inclination to catalyze the hydrogenation of various alkenes by molecular hydrogen [6]. Related to metal complexes of Schiff bases derived from salicylaldehyde, M(salens), are bis ortho naphtholimine metal complexes derived from 2-hydroxy-1-naphthaldehyde. A series of nickel(II) bis ortho naphtholimine complexes was synthesized and used for the catalytic hydrogenation of cyclohexene [8].

Hydrogenation of the unsaturated bond by the molecular hydrogen occurs by the molecular orbitals interaction between either the LUMO of C=C (π^*) with the HOMO of H₂ or LUMO of H₂ (σ^*) with HOMO of the C=C (π). However, these molecular orbitals have no net overlap, and therefore this reaction is "symmetry forbidden" and these symmetry limitations can only be overcome with the presence of a suitable catalyst.

Given the promising results in the hydrogenation of alkenes by these aforementioned palladium(II) complexes, the current work describes the synthesis and spectroscopic characterization of a novel series of bis ortho naphtholimine palladium(II) complexes. As well as study the catalytic hydrogenation of the mono olefin cyclohexene by the molecular hydrogen in presence of the prepared diimine palladium(II) chelates. Moreover, DFT calculations will be performed to correlate the structural properties of the existing palladium(II) complexes with their catalytic activity.

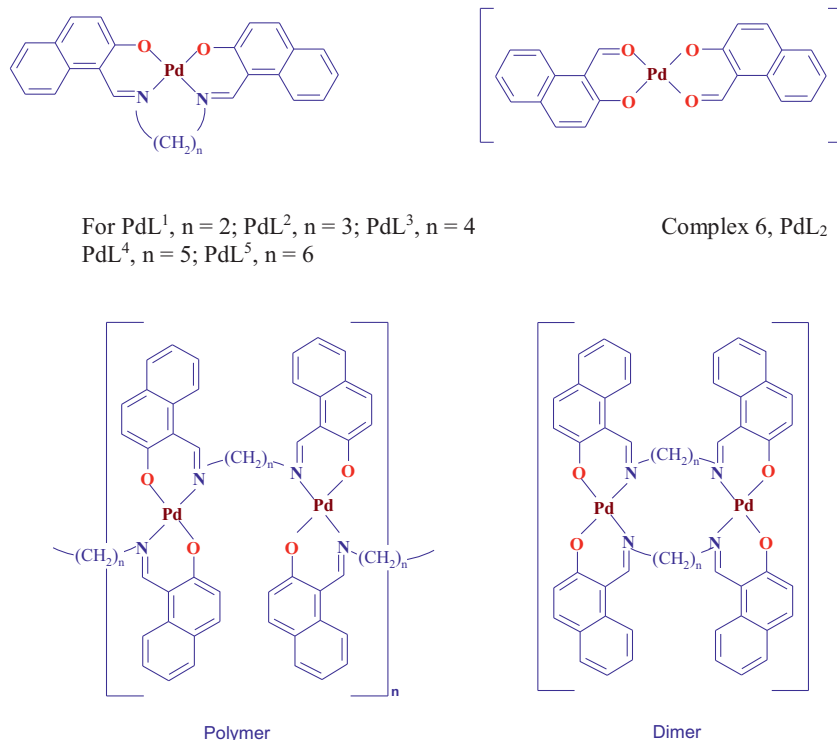
2. Experimental

2.1. Chemicals and Materials

The chemicals used in this work include organic materials and reagents, organic solvents and palladium(II) salt K₂[PdCl₄] are highly pure and were purchased from Sigma and Merck. 2-hydroxy-1-naphthaldehyde was purchased from Aldrich and was recrystallized from water before being used in the synthesis processes. The current Schiff base ligands were synthesized according to the method described in literature [9].

2.2. Synthesis of bis ortho naphtholimine palladium(II) complexes **1** and **2**

The used ligand (0.01 mole) was suspended in ethanol and refluxed for 1 hour, then aqueous solution of palladium(II) salt, K₂[PdCl₄], 0.01 mole was added slowly and the reaction mixture was refluxed with stirring for about 24 hours. After cooling, the green precipitate was filtered washed with ethanol, ether and then dried in vacuum. The dried green powder was further refluxed in a mixture of solvent (methanol and pyridine) in ratio (1:1) for about half hour. The cooling reaction mixture was filtered, washed with ethanol and finally dried in vacuum for one week. In the case of complex **1**, Pd^I, (see Scheme 1) the very fine green powder was recrystallized from nitrobenzene. Concerning complex **2**, (Pd^L²) the orange red crystal was obtained through recrystallization from the green powder in DMF. Concerning complexes **3**, **4** and **5** the direct interaction with palladium(II) ion and the Schiff base ligand was not convenient and the synthesis was achieved by reaction of the different diamines with bis-(2-OH-1-naphthaldehyde)-Pd(II) complex which was prepared as described below.



Scheme 1. Structures of palladium(II) complexes.

Table 1
Molecular formulae, physical properties, and elemental analysis of metal complexes 1-6.

Complex	Color	Crystal form	Solubility	Found (Calcd.)			
				%C	%H	%N	%M
1 PdL ¹	Brownish red	Plates	Nitrobenzene	60.93 (60.96)	3.81 (3.81)	5.93 (5.93)	22.60 (22.51)
2 PdL ²	Orange red	Needle	DMF	61.75 (61.67)	3.71 (4.11)	5.76 (5.76)	21.46 (21.87)
3 PdL ³	Canary yellow	Micocrystalline powder	CHCl ₃ , CH ₂ Cl ₂	62.93 (62.35)	5.00 (4.40)	6.40 (6.46)	21.15 (21.26)
4 PdL ⁴	Canary yellow	Micocrystalline powder	CHCl ₃ , CH ₂ Cl ₂	62.96 (62.98)	5.59 (4.67)	6.29 (5.45)	20.35 (20.68)
5 PdL ⁵	Canary yellow	Micocrystalline powder	CHCl ₃ , CH ₂ Cl ₂	63.17 (63.58)	5.25 (4.92)	5.58 (5.30)	19.83 (20.13)
6 PdL ₂ [*]	Reddish yellow	Micocrystalline powder	CHCl ₃ , CH ₂ Cl ₂	58.34 (58.82)	3.38 (3.56)	—	23.79 (23.72)

*L is 2-hydroxy-1-naphthaldehyde

2.3. Preparation of (2-OH-1-naphthaldehyde) palladium(II) complex 6

To a cold aqueous solution (30 ml) containing (0.006 mole) K₂[PdCl₄] 0.5 ml of concentrated HCl was added, and the solution was adjusted to pH = 5 - 6 by addition of 20 % aqueous solution of sodium acetate. Alcoholic solution of the recrystallized (several times) 2-OH-1-naphthaldehyde (0.012 mole) was added to the solution of palladium(II) ions and stirred. Yellow brown precipitate was formed immediately, which filtered, washed with (ethanol and H₂O) mixture and finally dried in vacuum. The crude yellow brown product was recrystallized from chloroform as yellow orange needles. The analytical results of bis-(naphthaldehyde) palladium(II) are reported in Table 1.

2.4. Synthesis of naphthalidimine palladium(II) complexes 3, 4 and 5

An equimolar amount of the different diamines dissolved in chloroform were added dropwise to the stirred solution of the crude product of bis-(naphthaldehyde) palladium(II) complex (0.2 mole) dissolved in chloroform. The reaction mixture was refluxed with stirring until the reactants were completely soluble. To separate the black powder palladium formed the reaction mixture solution was filtered. The resulting filtrate was evaporated under vacuum to reduce the volume of the solvent. On cooling and slow evaporation of solvent a yellow precipitate was formed. Addition of ether or petroleum ether was sometimes necessary to achieve complete precipitation. The yellow crude precipitate was recrystallized from chloroform to give pure canary yellow microcrystalline solid.

3.5. Conductometric Titration

The conductometric titrations carried out at room temperature by titrating 50 ml of 1×10^{-4} M of the palladium(II) ion solution using 0.5 ml increments of 1×10^{-3} M ligand solution. The electrical conductance values of the solutions were recorded after each addition and stirring the solutions for three minutes to allowing the equilibrium attainment. The specific conductivity of the solution was then corrected for volume change due to dilution effect, by multiplying the specific conductance, K, by the dilution factor, $(V_1 + V_2/V_1)$ where V₁ is the initial volume of the metal ion solution and V₂ is the ligand solution added. The obtained results were presented as XY curves as shown in supplementary material (S1). The stoichiometric ratios of the formed palladium(II) complexes in solution were determined from the breaks observed in the obtained curves.

2.6. Physical measurements

The physical measurements employed during the current study were performed as reported previously [8,10].

2.7. Catalytic hydrogenation study

2.7.1. Hydrogenation apparatus

The hydrogenation apparatus designed by Ohl [11] was used in the present study and described in the supplementary material (S2). This apparatus has the advantage, that it contains no mobile mechanical parts may be an undefined source of danger especially for long time reactions. In addition, all constructions can be achieved under the same conditions and also the sample can be change easily and fast. The total volume of the apparatus depends on the hydrogenation flask used and is about 3000 cm³.

2.7.2. Hydrogenation experiments

The current hydrogenation reactions were carried out using the apparatus described in S2. To remove the atmospheric oxygen, the hydrogenation apparatus containing the solution or suspension of the catalyst (2.6×10^{-3} M) in distilled DMF (80 ml) was flushed with argon for five minutes before each hydrogenation run. Thereafter, vacuum was applied until the mercury manometer read a height of 640 mm Hg. The pressure of the remaining argon was about 120 mm Hg. The hydrogen was then allowed to enter the apparatus until the total pressure of mercury was equal to 150 mm Hg. Then the cyclohexene (0.04 M) was added to the reaction medium from the storage container. Magnetic rapid stirring was applied to keep the reaction mixture mobile and to allow contact between the reactants. All the hydrogenation runs were carried out at room temperature in a time period of 150 hours. At the end of the reaction, argon was allowed again to enter the apparatus so that the pressure was equalized to the atmospheric one and then the sample required for analysis was taken out.

2.7.3. Analytical Process

At the end of each hydrogenation run, a 0.5 ml sample of the reaction mixture was taken for analysis. This 0.5 ml volume contained solvent, catalyst, cyclohexene and cyclohexane. The cyclohexene and the cyclohexane were separated from the other components by using a 2 cm Pasteur pipette filled with silica gel 60 (grain range 0.04 to 0.062 mm). In advance, the silica gel was activated in high vacuum for 4 hours at 220°C. 0.5 ml n-pentane was first allowed to pass through the Pasteur pipette, then, the 0.5 ml sample (taken directly from the hydrogenation flask) was feeded in the pipette and thereafter the pipette was flushed again with 0.5 ml n-pentane. The eluted solution contained a mixture of n-pentane, cyclohexene and cyclohexane. From this mixture 5 μ l was directly injected in the gas chromatograph device.

The quantitative analysis of the mixture was carried out using a Carlo Erba Instrument type 4200 connected with an integrator type SP 4100. The used detector was a flame ionization detector (FID), connected to the integrator through an electrometer (Carlo Erba Mod 180).

For the analysis, a 5 meter glass column was packed with alumina GC 80 to 100 MESH and conditioned for five days at 180°C in nitrogen stream (2.8 kg/cm²). Several runs of pure cyclohexene, cyclohexane, n-pentane and also their mixture with definite

Table 2
Thermogravimetric analysis of palladium(II) complexes 1-6.

Complex	T°C	DTA peaks	% Mass loss Found (Calcd.)	Species formed
1 PdL ¹	330 - 520	Exothermic	26.00(25.91)	PdO
2 PdL ²	340 - 370 370 - 570	Exothermic Exothermic	39.32(39.06) 25.79(25.16)	PdL _{0.5} PdO
3.PdL ³	280 - 330 330 - 540	Exothermic Exothermic	40.60(39.56) 21.50(24.45)	PdL _{0.5} PdO
4 PdL ⁴	190 - 355 355 - 545	Exothermic Exothermic	43.10(43.62) 22.50(23.79)	PdL _{0.45} PdO
5 PdL ⁵	290 - 359 395 - 570	Exothermic Exothermic	42.62(40.12) 20.50(23.16)	PdL _{0.5} PdO
6 PdL ₂ [*]	170 - 290 290 - 340 340 - 400	Exothermic Exothermic Exothermic	49.31(49.57) 07.08(07.63) 28.75(27.29)	PdL _{(1.35)}} PdL _{(0.75)}} PdO

*L is 2-hydroxy-1-naphthaldehyde.

concentrations were carried out in order to find out the optimum conditions for the analysis. According to these results the following conditions were: injector temperature 240°C, oven temperature 200°C, detector temperature 240°C, carrier gas N₂, and pressure of N₂ at working temperature is 2.8 kg/cm². Under these conditions, the total retention time of cyclohexane is 18 minutes and of cyclohexene 28 minutes. The injected 5 μL amount of the sample was small enough to prevent mutual influence of the components of the mixture, thus, constant retention times were observed in all measurements.

3. Results and Discussion

3.1. Characterization of palladium(II) Schiff base complexes

Two methods were employed to synthesize the current palladium(II) complexes based on the number of carbon atoms (n) of the methylene bridge (CH₂)_n between the diimine donor sites of the Schiff base ligands (Scheme 1). In the case of n = 2 or 3, the complexes were prepared through the direct interaction between Schiff base ligand and palladium(II) ion. Regarding Schiff base ligands with n = 4 - 6 the direct interaction with palladium(II) ion was inappropriate and the synthesis was achieved by reaction of the different diamines with the binary palladium(II) complex [PdL₂]; L is the ionized form of 2-OH-1-naphthaldehyde (HL). The molecular formulae of the pure isolated palladium(II) chelates are principally assigned in light of the results of the elemental and thermal analysis (Tables 1 and 2).

Comprehensive spectroscopic studies that include UV-Vis, IR, PXRD and X-ray single crystal completed the formulation of structures of the newly synthesized palladium(II) diimine complexes in question. Analytical results showed that the present metal chelates are free of water (coordination or surface) indicating that the coordination chromophore (N₂O₂) is provided entirely from existing donor sites of the diimine bases. In addition, the data in Table 1 indicate that the molar ratio for the reaction of palladium(II) ion with various Schiff bases is 1:1 (Pd:Schiff base). As shown in Table 1 the palladium(II) complexes obtained display varied solubility in organic solvents. All the complexes are also free of chloride anions in an indication that the existing Schiff bases are dibasic and the two phenolic protons of the ligand molecule are replaced by the palladium(II) ion during the complex formation.

The stoichiometry of the current diimine palladium(II) complexes formed under the prevailing experimental conditions is further supported by the results of conductometric titration of representative Schiff base ligands (H₂L) with palladium(II) ion solution. The conductance mole ratio curves (S1) display one break near the mole values of unity denoting the probable formation of one type of complexes (PdL). The conductometric titration curves are characterized by a marked increase of conductance with increasing the ligand concentration. This is due to the liberation of H⁺ from the phenolic groups of the ligand molecule, which replaced the much less conductive palladium(II) species in solution. A similar behavior was obtained in the case of 2-OH-1-naphthaldehyde as ligand but

the conductometric titration curve displays the break at the molar ratio of 1:2, which corresponds to the analytical data.

The melting point measurements of the present palladium(II) diimine complexes showed that these metal chelates were charred prior decomposition, indicating their thermal degradation without melting.

3.2. Thermal analysis (TGA and DTA)

The study of thermal analysis of metal complexes confirms the proposed molecular formulae based on the results of elemental analysis. The study of thermal analysis becomes important as it confirms the presence or absence of the water content in metal complexes and it also helps in identifying the nature of this content if it exists. In addition, the thermal investigation of metal complexes determines their thermal stability, especially if these metal chelates are used in catalytic processes at variable temperatures. Accordingly, the thermogravimetric and differential thermal analysis (TGA and DTA) of the palladium(II) diimine complexes under study was performed. Nitrogen is the inert atmosphere in which pyrolysis of palladium(II) complexes were measured. The temperature range in Celsius (°C) of the sequential thermal degradation steps with the weight loss percentage, and assignment the thermal fragments in addition to the corresponding DTA peaks are shown in Table 2. The corresponding TGA and DTA thermograms are present in Supplementary Material S3-S8.

With the exception of palladium(II) complex 1, it is observed that the pyrolysis patterns are very similar in the case of the other diimine palladium(II) complexes under investigation. Complex 1 is thermally degraded in one step to the corresponding metal oxide (PdO) while the other metal chelates degraded to the metal oxide in more than one step. In this context, the single-step pyrolysis of complex 1 occurs within the temperature range of 330 and 520 °C associated with very weak endothermic peak at 335 and a large one at 411 °C. Pyrolysis of complex 2 was performed in two steps between 334 and 565°C accompanied by three exothermic peaks, two weak at 334 and 362 and the other is strong and large at 495 °C. Typical pyrolysis pattern for complexes 3, 4 and 5 are as in the case of complex 2 but at lower temperature ranges. The thermograms of complexes 3, 4 and 5 exhibit two degradation steps with the temperature range of 240 to 540 °C associated with three exothermic peaks, located between 294 and 540 °C.

The existence of two steps as shown in S3-S9 denotes that the organic portion is first partially removed, giving an intermediate product, which is further decomposed to PdO. Despite the fact that the weight loss data (Table 2) indicate that the intermediate compound formed seems to contain half of the ligand, a clear understanding of the nature of this intermediate cannot be derived from these results of the TG analysis. This point would need further study.

For the binary complex, naphthaldehyde palladium(II) (PdL₂), the mode of pyrolysis seems to be even more complicated. Pyrolysis occurs in three decomposition stages in the temperature range from 180 to 400 °C. The first stage begins at 180 °C and the corre-

Table 3
FTIR spectra (cm⁻¹) of Schiff base ligands and their palladium(II) complexes(II).

Compound*	$\nu(\text{OH})$	$\nu(\text{C}=\text{N})$	$\delta(\text{OH})$	$\nu(\text{C}-\text{O})$	$\nu(\text{M}-\text{N})$	$\nu(\text{M}-\text{O})$
1 PdL ¹ L ¹	3440	1592 1616	- 1358	1392 1415	470	390
2 PdL ² L ²	3430	1593 1616	- 1355	1390 1415	480 -	405 -
3 PdL ³ L ³	3420	1590 1620	- 1360	1493 1420	495 -	402
4 PdL ⁴ L ⁴	3410	1575 1614	- 1373	1405 1435	480 -	380 -
5 PdL ⁵ L ⁵	3420	1590 1614	- 1370	1410 1450	478 -	383 -
6 PdL ₂ * L*	$\nu(\text{OH})$ - 3440	$\nu(\text{C}=\text{O})$ 1560 1631	$\delta(\text{OH})$ - 1377	$\nu(\text{C}-\text{O})$ 1407 1445	-	$\nu(\text{M}-\text{O})$ 385 -

*L is 2-hydroxy-1-naphthaldehyde.

sponding exothermic peak is located at the same value, 180 °C. In view of the significant mass loss value of 49.31% (Calcd. 49.57%), in this pyrolysis step, the initial removal of the organic portion begins early as compared to the corresponding Schiff base ligands. Two consecutive steps in the temperature range ranging from 290 to 410 °C accompanied by two exothermic peaks located at 304 and 381 that lead to volatilization of the rest of the organic part with the concomitant formation of PdO.

Some observations can be noted from the results of thermal measurements, which can be summarized as follows:

1- Although complexes **2-5** show similarity in their pyrolysis pattern the first step in the case of complex **2** begins at temperature values higher than in the case of complexes **3, 4** and **5**. This finding is in line with the increased length of the carbon chain between the two Schiff base linkages of the diimine ligands. The direction of the temperature value for the start of the first step follows the order **5** < **4** < **3** < **2** \approx **1** as shown in Table 2.

2- The values of the palladium content calculated from PdO residue are in a good agreement with the experimental metal values for the molecular formulas recorded in Table 1.

3- The DT curves shown in (S3-S9) contain obvious exothermic peaks corresponding to the various decomposition steps of the TG curves. The absence of endothermic peaks in the DT curves denotes that the proposed complexes do not undergo melting or suffer any lattice changes before decomposition. This is in agreement with the observation that all the prepared complexes in this work decompose without melting.

3.3. Infra red spectra and mode of bonding

The mode of bonding of the present diimine ligands to the palladium(II) ion is best easily verified by studying the IR spectra of the complexes in comparison with those of the ligands. In this regard the spectral interpretation data is included in Table 3 as they are obtained from the corresponding charts given in S9-S20. The specific symmetric and asymmetric vibrations of $\nu(\text{OH})$ appears as a medium broad peak within the wavenumber range of 3410 - 3440 cm⁻¹, while the other types of the characteristics frequencies of OH group such as $\delta(\text{OH})$ and $\gamma(\text{OH})$ appeared as intense peaks at 1355 - 1373 and 820 - 850 cm⁻¹ respectively [12]. The data in Table 3 indicate that the characteristics frequencies of the OH-group of the current diimine ligands are vanished in the spectra of the corresponding palladium(II) complexes [8]. This indicates the elimination of the hydrogen of the OH groups when the ligands interacted with the palladium(II) ion to form the metal complex. The disappearance of the different characteristics frequencies of the OH group from spectra of palladium(II) complexes is similar to those previously reported for the corresponding nickel(II) diimine complexes [8]. The bonding of the phenolic oxygen to palladium(II) ion is also inferred from the shift of the $\nu(\text{C}-\text{O})$ band at 1415 - 1450 cm⁻¹ to lower wavenumbers (1390 - 1405 cm⁻¹) in the spectra of the complexes as a result of the increased mass of the group attached to the carbon atom being now C-O-Pd instead of C-O-H [12]. This lowering of the band frequency indicates also obvious covalent bonding between the oxygen and palladium(II) ion. It should

be noted that the consistent spectral data confirm that the palladium(II) complexes are free of solvent molecules, which is consistent with assigned molecular formulae based on the results of elemental and thermal analysis.

The participation of the azomethine nitrogen in coordination to palladium(II) ion is evident from the observed shift of $\nu(\text{C}=\text{N})$ to lower wavenumbers with values from 23 to 30 cm⁻¹ in the spectra of the metal complexes (Table 3) [13]. Accordingly, the current diimine ligands are coordinate to the palladium(II) ion, as dibasic tetradentate ligands [13]. Bonds involving the azomethine nitrogen and the phenolic oxygen to palladium(II) center are confirmed by the appearance of the two new bands within the wavenumber ranges of 470 - 495 and 380 - 405 cm⁻¹ designated for $\nu(\text{M}-\text{N})$ and $\nu(\text{M}-\text{O})$ respectively [12].

With respect to complexes **1** and **2** the coordination chromophore sites, N₂O₂, are provided by only one naphthaldiimine molecule, since this type of interaction leads to formation of five or six membered chelate rings. As regards diimine palladium(II) chelates with more than three carbon atoms in the bridged chelate ring would be rather unstable (Scheme 1). This is because the four donor sites, N₂O₂, cannot be provided by only one ligand molecule to the palladium(II) ion. Thus complexes **3 - 5** can only be formed as dimeric or polymeric complexes as shown in Scheme 1.

Comparing the spectra of both the free 2-OH-1-naphthaldehyde and its palladium(II) complex (PdL₂), revealed some changes that include: disappearance of the various OH bands at 3440, 1377 and 830 cm⁻¹ assignable to $\nu(\text{OH})$, $\delta(\text{OH})$, and $\gamma(\text{OH})$ respectively [12]. As well the shift of the $\nu(\text{C}=\text{O})$ band at 1631 cm⁻¹ in the spectrum of the free 2-OH-1-naphthaldehyde to lower wavenumber (1560 cm⁻¹) in the spectrum of PdL₂ confirms coordination of the carbonyl oxygen to palladium(II) ion. These spectral features are a clear reference to the bonding of 2-OH-1-naphthaldehyde ligand to palladium(II) ion through the deprotonated phenolic oxygen and the aldehydic carbonyl oxygen [12].

In light of the above-mentioned results, which include elemental and thermal analysis, as well as spectral investigations, the diimine palladium(II) complexes under study can be formulated as shown in Scheme 1.

3.4. Electronic absorption spectra

Magnetic moment determinations at room temperature demonstrated that the current palladium(II) complexes are diamagnetic and hence they must be in the low-spin state of the square planar configuration. Metal complexes of d⁸- elements of the coordination number four in the low spin configuration are square planar stereochemistry characterized by three spin-allowed d-d transitions that are: $d_{xy}(b_{2g}) \rightarrow d_{x^2-y^2}(b_{1g})$, $d_z^2(a_{1g}) \rightarrow d_{x^2-y^2}(b_{1g})$, and $d_{xz,yz}(e_g) \rightarrow d_{x^2-y^2}(b_{1g})$ related to ${}^1A_{1g} \rightarrow {}^1A_{2g}$, ${}^1A_{1g} \rightarrow {}^1B_g$, ${}^1A_{1g} \rightarrow {}^1E_{1g}$ respectively [14].

A suitable single crystal for X-ray structural analysis was successfully obtained only in the case of complex **2**. Accordingly comparative spectral measurements were carried out and linked to complex **2** (see section 3.5.) to elucidate the stereochemistry of the other palladium(II) complexes under study. In this regard, the spec-

Table 4
Electronic absorption spectra of palladium(II) complexes **1-6**.

Complex	Observed band (cm ⁻¹)	Assignments
PdL ¹	16400	¹ A _{1g} → ¹ A _{2g}
	18000	¹ A _{1g} → ¹ B _g
	19400	¹ A _{1g} → ¹ E _{1g}
PdL ¹ , PdL ² , PdL ³ , PdL ⁴ , PdL ⁵ , PdL ^{2*}	22727	Ligand and c.t.
	26315	
	28200	
	33898	
	40000	Aromatic transition π → π*
	22727 – 24096	Ligand and c.t.
	25974 – 26300	
	31250 – 37037	Aromatic transition π → π*
	40000 – 42553	

*L is 2-hydroxy-1-naphthaldehyde

tra of the current palladium(II) complexes were measured in the solid state as KBr disc in the ultra violet and visible region. The recorded spectra of the palladium(II) complexes shown in S21-S22 are similar indicating that their stereochemistries are alike. Since X-ray structural analysis of complex **2** confirms square planar environment around palladium(II) ion therefore we suggest square-planar stereochemistry for the other palladium(II) complexes under study.

The bands related to the excitation of the d-electrons on the palladium(II) ion are observed with satisfactory intensity only in the case of complex **1**. The highest energy d-d band at 19400 cm⁻¹ can be assigned to d_{xz,yz}(e_g) → d_{x²-y²}(b_{1g}) transition corresponding to the ¹A_{1g} → ¹E_{1g} state. The band at 18000 cm⁻¹ is due to the d_{z²}(a_{1g}) → d_{x²-y²}(b_{1g}) transition represented by the ¹A_{1g} → ¹B_g (ν₂) state, while the shoulder at 16400 cm⁻¹ originates from the d_{xy}(b_{2g}) → d_{x²-y²}(b_{1g}) transition corresponding to the ¹A_{1g} → ¹A_{2g} (ν₁).

The values of orbital energy differences Δ₁, Δ₂ and Δ₃ are 18100, 3200 and 1100 cm⁻¹ respectively have been evaluated using the assumption that: F₂ = 10F₄ = 600 cm⁻¹ for a Salter Condon interelectronic repulsion [15]. The separation Δ₁ was the largest which indicated that the d_{x²-y²} was strongly antibonding. Also from the observed spectral data of complex **1**, the ν₂/ν₁ ratio is (1.09), which is in close agreement with that reported for square planar complexes [16]. The spectrum of naphthaldehyde palladium(II) complex **6** displays only one d-d band at 21500 cm⁻¹ could be due to the ¹A_{1g} → ¹E_{1g} transition while other bands of d-d transitions are too weak to be observed.

The observed strong and intense bands within the 37037–42553 cm⁻¹ rang are assignable to the π → π* transitions of the aromatic ring and the intermolecular charge transfer (c.t.) interaction while the d - d transitions of the palladium(II) ion are rather poor. In addition weak new absorption bands attributable to ligand to metal interaction appeared within the wavenumber range of 22727–33898 cm⁻¹, Table 4.

The origin of the poor electronic absorption spectra of the current palladium(II) complexes may arise from the fact that the bands due to d-d transitions of the palladium(II) ion interact strongly with those of the internal ligand c.t. and metal to ligand c.t. bands. This can be confirmed by the observation that complex formation between palladium(II) ions and the diimine or naphthaldehyde ligands does not lead to pronounced changes in color, hence the electronic visible spectra would not be much different. The same finding was reported for the d-d bands of palladium(II) Schiff bases that are masked by the intense ligand c.t. bands [17].

3.5. X-ray single crystal structural analysis

For the diimine palladium(II) complex **2** (Scheme 1), proper single crystals were obtained for a complete structure determination

Table 5
Crystal data and structure refinement of naphthaldehyde palladium(II) complex **2**.

Empirical formula	C ₂₅ H ₂₀ N ₂ O ₂ Pd
Formula weight	486.83
Temperature/K	150.00(10)
Crystal system	monoclinic
Space group	P2 ₁ /n
a/Å	14.4372(4)
b/Å	8.2588(2)
c/Å	16.4604(5)
α/°	90
β/°	101.122(3)
γ/°	90
Volume/Å ³	1925.78(9)
Z	4
ρ _{calc} /g/cm ³	1.679
μ/mm ⁻¹	0.990
F(000)	984.0
Crystal size/mm ³	1.042 × 0.375 × 0.312
Radiation	Mo Kα (λ = 0.71073)
2θ range for data collection/°	7.058 to 60.666
Index ranges	-20 ≤ h ≤ 20, -9 ≤ k ≤ 11, -23 ≤ l ≤ 23
Reflections collected	18625
Independent reflections	5105 [R _{int} = 0.0318, R _{sigma} = 0.0364]
Data/restraints/parameters	5105/0/271
Goodness-of-fit on F ²	1.052
Final R indexes [I > 2σ (I)]	R ₁ = 0.0276, wR ₂ = 0.0548
Final R indexes [all data]	R ₁ = 0.0355, wR ₂ = 0.0581
Largest diff. peak/hole / e Å ⁻³	0.45/-0.39

Table 6
Bond angles (°) experimental and theoretical of palladium(II) complex **2**, (PdL²).

Experimental (τ ₄ = 0.126)	Theoretical* (τ ₄ = 0.118)	Δ
O1 – Pd – O2	80.42	01 – Pd – O2 80.4822 0.0622
O1 – Pd – N1	90.83	01 – Pd – N1 90.8497 0.01970
O1 – Pd – N2	171.30	01 – Pd – N2 171.7242 0.4242
O2 – Pd – N1	171.02	02 – Pd – N1 171.7127 0.6927
O2 – Pd – N2	91.20	02 – Pd – N2 90.8937 0.3063
N1 – Pd – N2	97.63	N1 – Pd – N2 97.5393 0.0907

*Values determined from DFT calculations (see section 3.7.). The labeling of the atoms in the third column can be related to those of S26 as follows: O1, O2, N1 and N2 correspond to O41, O19, N40 and N20 respectively.

by X-ray diffraction. The obtained crystallographic information are presented in Table 5, and the more relevant bond lengths and bond angles are given in Tables 6 and 7, respectively while the numbering scheme adopted is shown in Fig. 1. The data in Table 5 display that crystals belong to the monoclinic space group P2₁/n with the lattice data a = 14.34426 Å, b = 12.96501 Å, c = 5.50817 Å, α = 90°, β = 95.293° and γ = 90°. The molecular structure consists of discrete molecules of which four are in the unit cell as

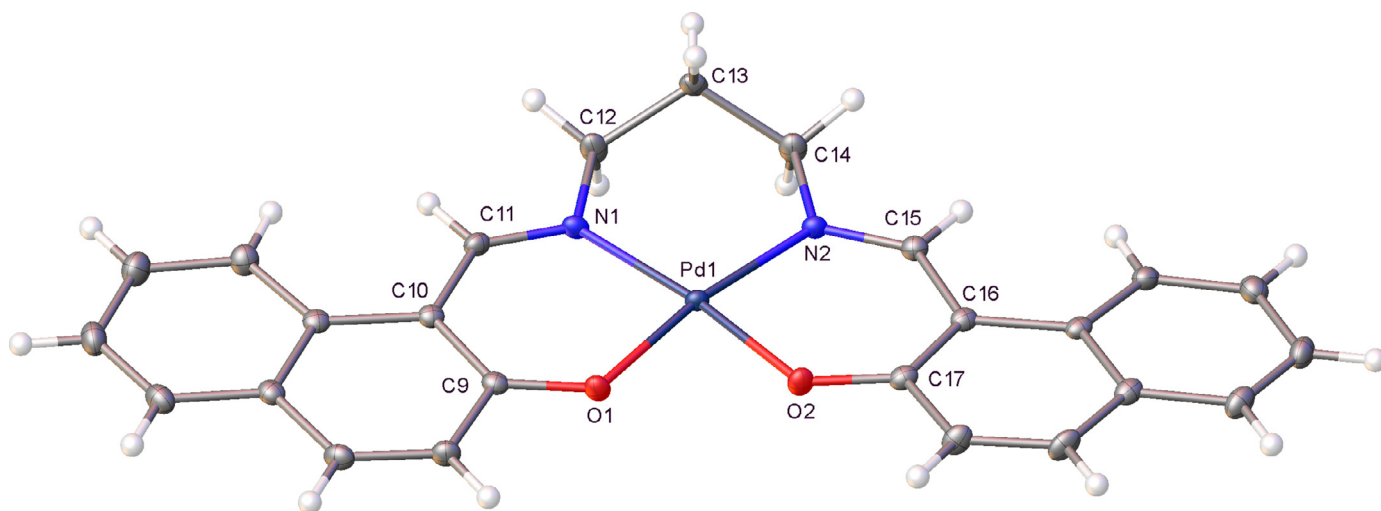


Fig. 1. Presentation of the single crystal X-ray structure of palladium(II) complex **2**, showing the labeling scheme of non-hydrogen atoms.

Table 7

Bond lengths (Å) experimental and theoretical of palladium(II) complex **2**, (PdL²).

	Experimental	Theoretical*		Δ
Pd1 – O1	1.9828	Pd1 – O1	2.027	0.0442
Pd1 – O2	1.9905	Pd1 – O2	2.0271	0.0366
Pd1 – N1	2.0073	Pd1 – N1	2.0213	0.0140
Pd1 – N2	2.0021	Pd1 – N2	2.0212	0.0191

*Values determined from DFT calculations (see section 3.7.). The labeling of the atoms in the third column can be related to those of S26 as follows: O1, O2, N1 and N2 correspond to O41, O19, N40 and N20 respectively.

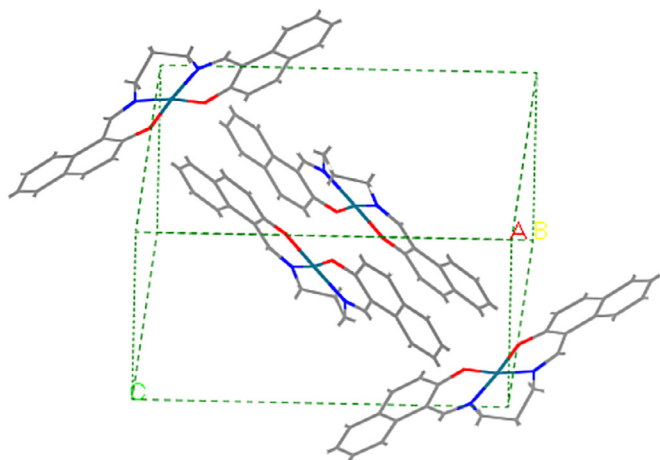


Fig. 2. A packing diagram of the complex **2**.

shown in Fig. 2; accordingly no atoms are required to be in special position.

Except for the middle carbon atom of the propylene bridge the molecules are nearly planar, with the tetra coordinated palladium(II) ion in the center. The coordination polyhedron around palladium(II) center is occupied by the quadridentate chromophore N₂O₂, provided by the donor atoms O(1), O(2), N(3) and N(4) of the diimine ligand. The question that arises now is how the present X-ray data distinguish between the tetrahedral and square planar stereochemistry of the four-coordinated palladium(II) complex. The answer to this question comes from defining the four-coordinate geometrical index $\tau_4 = [360 - (\alpha + \beta)]/141$ (α and β

are the two largest angles around the metal center) [18]. In this context, if τ_4 is 1 the hybridization of palladium(II) ion is sp³ for a perfect tetrahedron geometry while for a perfect square planar stereochemistry τ_4 equals zero and the corresponding hybridization is dsp² [18].

The specific value of τ_4 is 0.126 that indicates square planar geometry slightly distorted in consistency with magnetic and spectroscopic investigations.

The results of the X-ray single crystal structural analysis of [N,N'-propylene-bis-(naphthaldehyde)] palladium(II) complex (PdL²), are compared with data obtained for the analogous salen complexes. These complexes are [N,N'-ethylene-bis-(salicyaldimine)] nickel(II) (NiL¹) [19] [N,N'-propylene-bis-(salicyaldimine)] nickel(II) (NiL²) [20] and [N,N'-ethylene-bis-(salicyaldimine)] platinum(II) (PtL¹) [21]. For both salen complexes, (NiL¹) and (PtL¹), the overall structure is nearly planar, as in the case of (PdL²). On the other hand, for the brown crystal of NiL² the coordination geometry is tetrahedral in consistency with the sp³ hybridization of the paramagnetic d⁸ nickel(II) ion while PtL¹ is diamagnetic with dsp² hybridization of d⁸ platinum(II) center in the square planar environment. In the same vein, for the reported two salen nickel(II) complexes NiL¹ and NiL² the later (NiL²) is brown and paramagnetic with tetrahedral geometry while NiL¹ is green and diamagnetic with square planar structure. These findings indicate that, despite the overall structural similarity between these diimine metal complexes nevertheless, there are quite characteristic differences in the geometrical environment of the central metal ions, dependent on the length of the alkane bridge between the two nitrogen donors.

For the present palladium(II) complex **2** the metal oxygen distances, Pd1–O1 and Pd1–O2, are 1.9828 and 1.9905 Å respectively. As well the palladium(II) nitrogen bond lengths, Pd1–N1 and Pd1–N2, are 2.0073 and 2.0021 Å respectively. These lengths of bonding between the metal and both oxygen and nitrogen atoms are in the normal values for these types of metal complexes as shown in Table 8 and others [22].

For the metal complexes with the ethylene bridge, NiL¹ and PtL¹, the O–M–N angle is widened to be about 94.4°, to reduce the strain in the six membered chelate rings N–C–C–O, whereas a N–M–N angle of 84.6 – 85.0° is enough to fit with normal tetrahedral angles at the bridging carbon atoms. But in the case of NiL² and PdL² complexes that contain the three carbon atoms of the propylene bridge the bond angle N–M–N has expanded to over 90° at the expense of compression the bond an-

Table 8
Bond angles (°) and lengths (Å) of Ni(II), Pd(II) and Pt(II) of diimine complexes.

Bond angles (°)	PdL ²	NiL ²	NiL ¹	PtL ¹
O-M-O	80.42	83.0	85.5	86.8
N-M-N	97.63	92.4	85.0	84.6
O-M-N	91.20, 90.83	93.4, 94.1	94.3, 94.5	94.3
M-O-C _R	128.83, 128.30	125.5, 126.8	129, 128	123.8
M-N-C _R	123.51, 123.11	126.2, 125.1	126, 126	127.0
M-N-C _B	121.11, 121.15	116.7, 117.0	116, 113	113.7
N-C _B -C _B	113.23, 113.46	110.2, 114.0	107	109.7
C _B -C _B -C _B	113.03	113.6
N-C-C _R	130.09, 130.15	123.1, 124.6	125, 127	124.1
O-C _R -C _R	125.55, 125.44	122.3, 122.5	123, 124	125.1
C-C _R -C _R	120.93, 121.13	124.2, 124.1	122, 119	125.5
Bond lengths (Å)				
M-O1, M-O2	1.9828, 1.9905	1.868, 1.838	1.89, 1.830	1.989
M-N1, M-N2	2.0073, 2.0021	1.854, 1.868	1.870, 1.850	1.934
N-C _B	1.477, 1.478	1.508, 1.468	1.500, 1.460	1.502
C _B -C _B	1.502, 1.508	1.512, 1.530	1.520, 1.520	1.474
C-O	1.290, 1.299	1.312, 1.310	1.300, 1.310	1.319
N=C	1.294, 1.301	1.307, 1.288	1.290, 1.280	1.287
C _R -C _R	1.431, 1.430	1.400, 1.371	1.440, 1.440	1.442
C _R -C _R	1.431, 1.407	1.391, 1.383	1.440, 1.440	1.429

PdL² is [N,N'-propylene-bis-(naphthalaldimine)]palladium(II); NiL² is [N,N'-propylene-bis-(salicyaldimine)]nickel(II); NiL¹ is [N,N'-ethylene-bis-(salicyaldimine)] nickel(II); PtL¹ is [N,N'-ethylene-bis-(salicyaldimine)] platinum(II), B = bridge; R = chelate ring

gle O-M-O to 80.42 - 83°. In the same regard the O-M-N angles tend to be reduced, exerting additional strain in the six membered chelate ring (N-C-C-O) containing the alkyl propylene bridge.

With the smaller nickel(II) center, a considerable tetrahedral distortion was observed [20], reducing this strain with the propylene chain connecting the two nitrogen atoms. With the largest palladium(II) ion present, the system remains almost flat, but the angles between both the oxygen atoms bound to the naphthalene carbon atoms are opened up to 128.30 and 128.83°. In the same context the bond angles between the nitrogen atoms and the linked carbon atoms of the propylene bridge are widened to 123.11 - 126.20°. In this case even the bridging carbon linked to nitrogen stay in the plane, and only the middle carbon atom of the propylene bridge is tilted to one side. However, even with all these distortions, the ring angles on all carbon atoms of the bridge in both the nickel(II) and the palladium(II) complexes are widened to 116.7 - 121.15° which will cause additional strain for the whole system.

With respect to the naphthyl group, the findings are very similar to naphthalene itself with respect to the carbon and carbon atoms distances and angles. As regards the C=N bond distance (1.287 - 1.294 Å) it is somewhat longer than expected for a normal double bond. In the same regard the C-O distance (1.220 - 1.319 Å) is considerable shorter than for the phenolic OH group. The same thing is observed in the case of the linkage of the imine carbon atom to the phenyl ring (1.431 Å) indicating some double bond character as well.

This is consistent with the participation of the oxygen atom and the C=N group in the resonance of the aromatic system, and with all findings for this type of metal complexes. For both C-O and C=N, the differences in the lengths of these bonds for the metal complexes being examined are minimal and can be ignored, as is evident from the data in Table 8.

3.6. PXRD structural analysis

With the exception of complex **2**, several attempts were made to develop single crystals suitable for X-ray diffraction measurements to determine the exact structure of the existing diimine palladium(II) complexes, but they were unsuccessful. Otherwise, an

appropriate reddish-orange microcrystalline samples were isolated by recrystallization of the palladium(II) complex **1**, PdL¹, from nitrobenzene. In the case of the naphthaldehyde palladium(II) complex **6**, PdL₂, radish-yellow microcrystalline powder was obtained by recrystallization from chloroform.

Recently, treatment of the results of X-ray powder diffraction measurements using some computer programs to prove the final and accurate structure of the metal complexes is a scientific approach that has proven to be applicable [10,23]. In this context, the Expo 2014 program is the most applied in treating the results of X-ray powder diffraction measurements to demonstrate the accurate and final structure of metal complexes depending on the Rietveld methodology [24]. Strong verification of the crystal structure of the metal chelates can be obtained from PXRD data processing through the Rietveld approach [23,24].

PXRD spectral patterns for the palladium(II) complexes **1** and **6** are illustrated in Fig. 3 and S23. The accuracy of the compatibility between theoretical calculations and the experimental data of measuring X-ray diffraction for the microcrystalline powder of complexes **1** and **6** in the final Rietveld Refinement is shown in Fig. 4 and S24 respectively. Crystalline data, the most relevant chosen bond distances, and bond angles of the palladium(II) complexes **1** and **6** are found in Tables 9, 10 and 11 while the approved numbering schemes are shown in Figs. 5 and 6.

The data in Table 9 reveals that the crystalline system of both complexes **1** and **6** is triclinic and the corresponding space group is P-1. With respect to complex **1**, the dimensions of the unit cell *a*, *b* and *c* are 11.48254, 9.45613, and 5.28965 Å respectively with the corresponding $\alpha = 90.911^\circ$, $\beta = 90.671^\circ$ and $\gamma = 95.216^\circ$. In the case of complex **6** the characteristic unit cell dimensions are 13.38400, 7.88922 and 6.87570 Å for *a*, *b* and *c* respectively along with the α , β and γ angles in the order values of 107.701°, 104.851° and 75.357°.

Figs. 5 and 6 demonstrate that the coordination chromophore around the palladium(II) center consists of N₂O₂ and O₄ in the case of complexes **1** and **6** respectively.

The coordination polyhedron of these palladium(II) centers was deduced from the geometrical index τ_4 . As mentioned previously for palladium(II) **2**, τ_4 was determined to be 0.126 while in the case of complexes **1** and **6** the determined values of τ_4 were 0.0539 and 0.0027, respectively (see Tables 10 and 12). These values of the geometrical index refer to square planar stereochemistry for the four coordinated palladium(II) complexes in question. This finding is further confirmed from the values of bond angles and distances between the d⁸-metal(II) center and both oxygen and nitrogen donor atoms which are in the normal values for these types of square planar metal complexes [11,19,25].

3.7. Density function theory (DFT) study

Computer chemistry calculations allow access to the ideal molecular stereochemistry for a metal complex molecule comparable to those obtained by X-ray measurements. All calculations were carried out using DFT as performed with Gaussian 09 [26]. For this purpose, the B3LYP hybrid approach [27] was used for the molecular geometrical optimization determinations in the case of palladium(II) complexes **1**, **2**, **3** and **6** under study. All the calculations were carried out with applying the LANL2DZ effective core potential basis set on Pd, and 6-31G basis set on all other elements. With regard to complexes **1**, **2**, and **6**, their geometrical optimization determination was already achieved by X-ray structural analysis measurements as discussed in the previous section.

The purpose of the DFT study of these palladium(II) complexes is to correlate their structural properties and the catalytic activity towards the hydrogenation of cyclohexene and the obtained results are summarized in Table 18. In addition, the optimized ge-

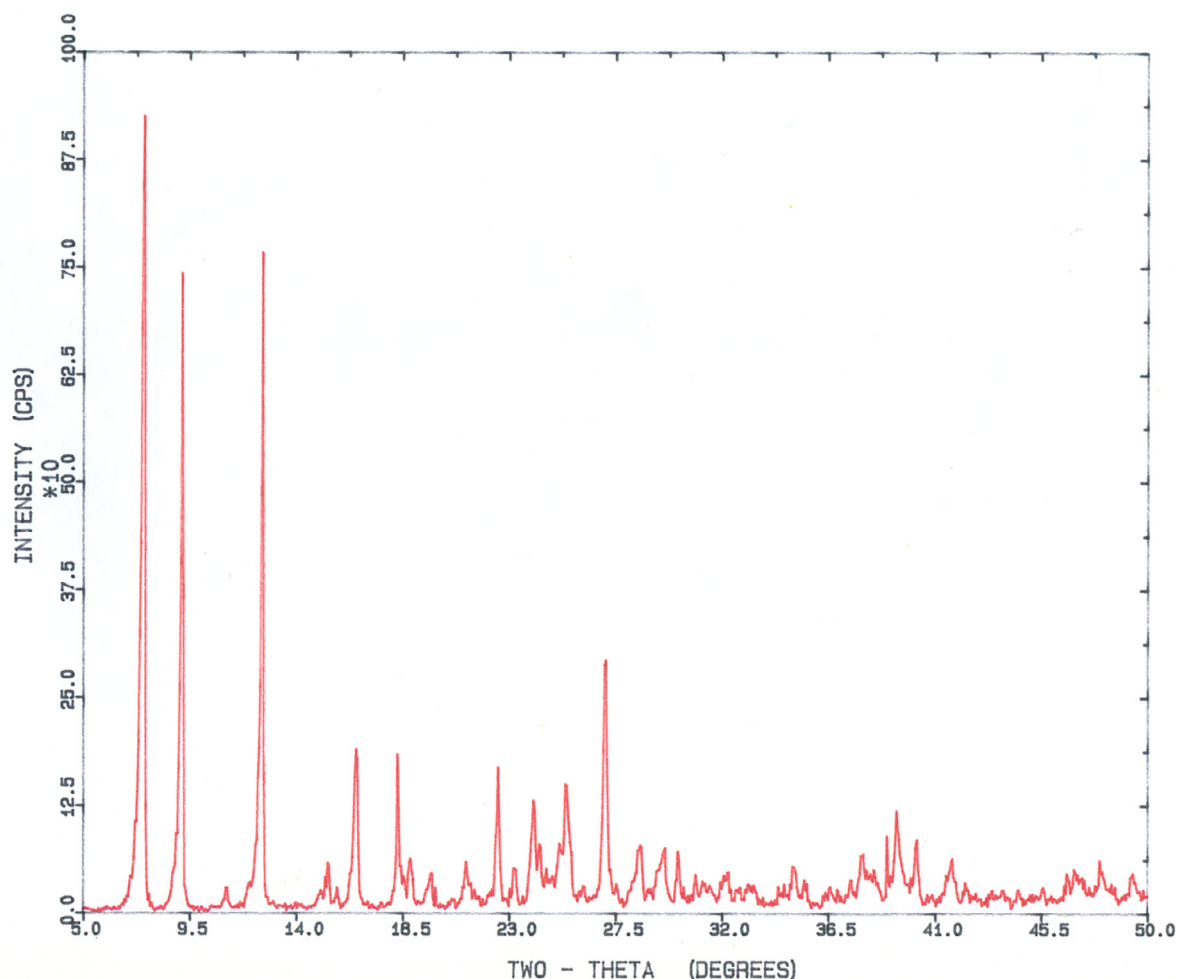


Fig. 3. The powder XRD pattern of complex 1.

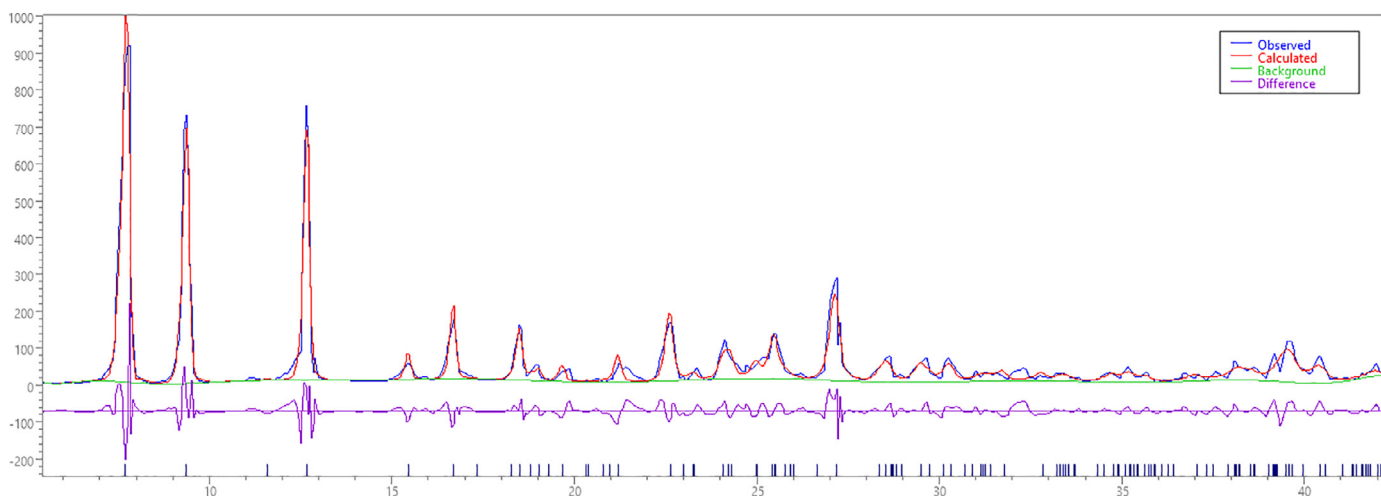


Fig. 4. The good match between the practical and calculated data of PXRD patterns based on Rietveld Refinement of complex 1.

ometrical parameters deduced from the X-ray measurements for structural analysis are compared with the corresponding ones obtained by DFT calculations in the case of complexes **1**, **2** and **6**. In this regard the relevant bond lengths and bond angles in addition to the geometrical index τ_4 are compared with computationally optimized parameters as shown in Tables 6,7,10-13, while the approved numbering schemes are given in the S25-S28. The data

in Tables 6,7,10-13 display excellent matches between the experimental and calculated values of the optimized geometrical parameters. This finding provides a reliable test for the accuracy of the current computationally geometrical optimization of palladium(II) complexes.

With respect to complex **3**, DFT calculations were carried out to decide the most appropriate molecular structure as well as to

Table 9
Crystallographic data of palladium(II) complexes **1** and **6**.

Complex	PdL ¹ (1)	PdL ₂ [*] (6)
Empirical formula	PdC ₂₄ H ₁₈ N ₂ O ₂	PdC ₂₂ H ₁₄ O ₄
Formula weight	472.42	448.4
T (K)	295	295
λ (Å)	1.52904	1.529040
Crystal system	Triclinic	Triclinic
Space group	P -1	P -1
Centro symmetry	Centric	Centric
Space Group Number	2	2
Unit cell dimensions:		
a (Å), b (Å), c (Å)	11.48254; 9.45613, 5.28965	13.38400, 7.88922, 6.87570
α (°), β (°), γ (°)	90.911, 90.671,	107.701, 104.851, 75.357
Cell volume (Å ³)	90.671,	95.216 571.85 22.87 0.87
Volume per atom (Å ³)		5.342 – 42.172 731 8.726
Calculated density (g/cm ³) θ		24.381 1.044 1.240
range for data collection (°)		
Total reflection Rietveld results: Rp Rwp R-Bragg R-F		

*L is 2-hydroxy-1-naphthaldehyde

Table 10Bond angles (°) of palladium(II) complex **1**, (PdL¹) experimental and theoretical.

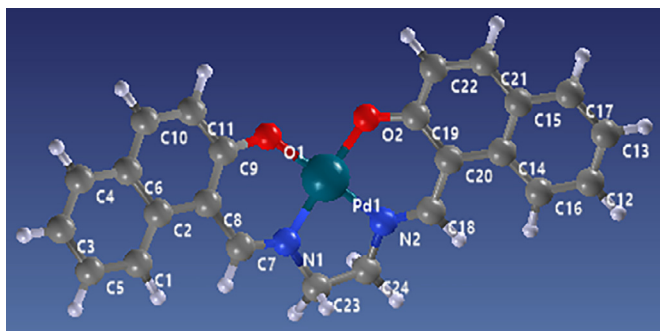
Experimental (τ ₄ = 0.0539)	Theoretical* (τ ₄ = 0.0545)	Δ
N1 – Pd1 – O1	91.45	N1 – Pd – O1 91.313 0.137
N1 – Pd1 – N2	84.93	N1 – Pd – N2 85.0896 0.1596
N1 – Pd1 – O2	176.33	N1 – Pd – O2 176.1822 0.1478
N2 – Pd1 – O1	176.12	N2 – Pd – O1 176.1819 0.0619
O1 – Pd1 – O2	91.49	O1 – Pd – O2 91.3129 0.1771
N2 – Pd1 – O2	92.17	N2 – Pd – O2 92.3113 0.1413

*Values determined from DFT calculations (see section 3.7.). The labeling of the atoms in the third column can be related to those of S25 as follows: O1, O2, N1 and N2 correspond to O19, O41, N20 and N40 respectively.

Table 11Bond lengths (Å) of palladium(II) complex **1**, (PdL¹) experimental and theoretical.

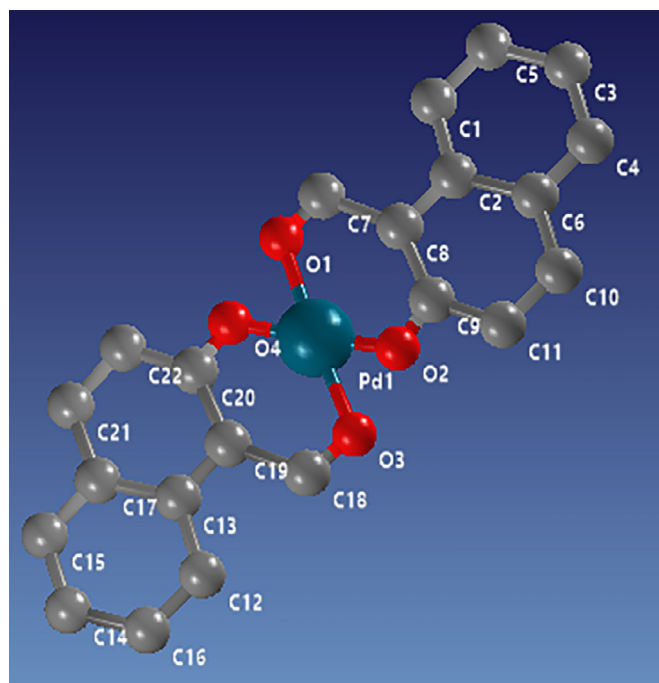
Experimental	Theoretical*	Δ
O1 – Pd	1.895775	O1 – Pd 2.0282 0.1324
O2 – Pd	1.893685	O2 – Pd 2.0282 0.1345
N1 – Pd	1.970088	N1 – Pd 1.9873 0.1172
N2 – Pd	1.946273	N2 – Pd 1.9873 0.0410

*Values determined from DFT calculations (see section 3.7.). The labeling of the atoms in the third column can be related to those of S25 as follows: O1, O2, O3 and O4 correspond to O19, O41, N20 and N40 respectively.

**Fig. 5.** The optimized structure of naphthalaldimine palladium(II) complex **1**.

determine its optimized geometry. In this context computationally geometrical optimization were performed for both the monomeric (see S27) and dimeric structure (Fig. 7) of this metal chelate.

The total energy calculated by DFT method which composed of the internal, potential, and kinetic energy is a profitable pa-

**Fig. 6.** The optimized structure of 2-hydroxy-1-naphthaldehyde palladium(II) complex **6**.

rameter. The total energy (E) values calculated for dimeric structure for complex **3** is – 1745218.13123139 Kcal/mole, while for the monomer structure is – 872617.258729406 Kcal/mole. The difference in bonding energy of the monomer from the dimer = – 1745218.13123139 – 2 × – 872617.258729406 = 16.4 Kcal/mole. This finding can be attributed to the fact that, for the monomer structure, the chelating ring of the alkyl bridge between two donors of azomethines is greater than six, and this causes the compound to become strained. The most stable optimized dimeric structure of the palladium(II) chelate **3** is illustrated in Fig. 7 and selected bond angles and bond distances are listed in Tables 14 and 15. Based on the calculated values of the geometrical index τ₄ the coordination polyhedrons around both palladium(II) centers are square planar environment.

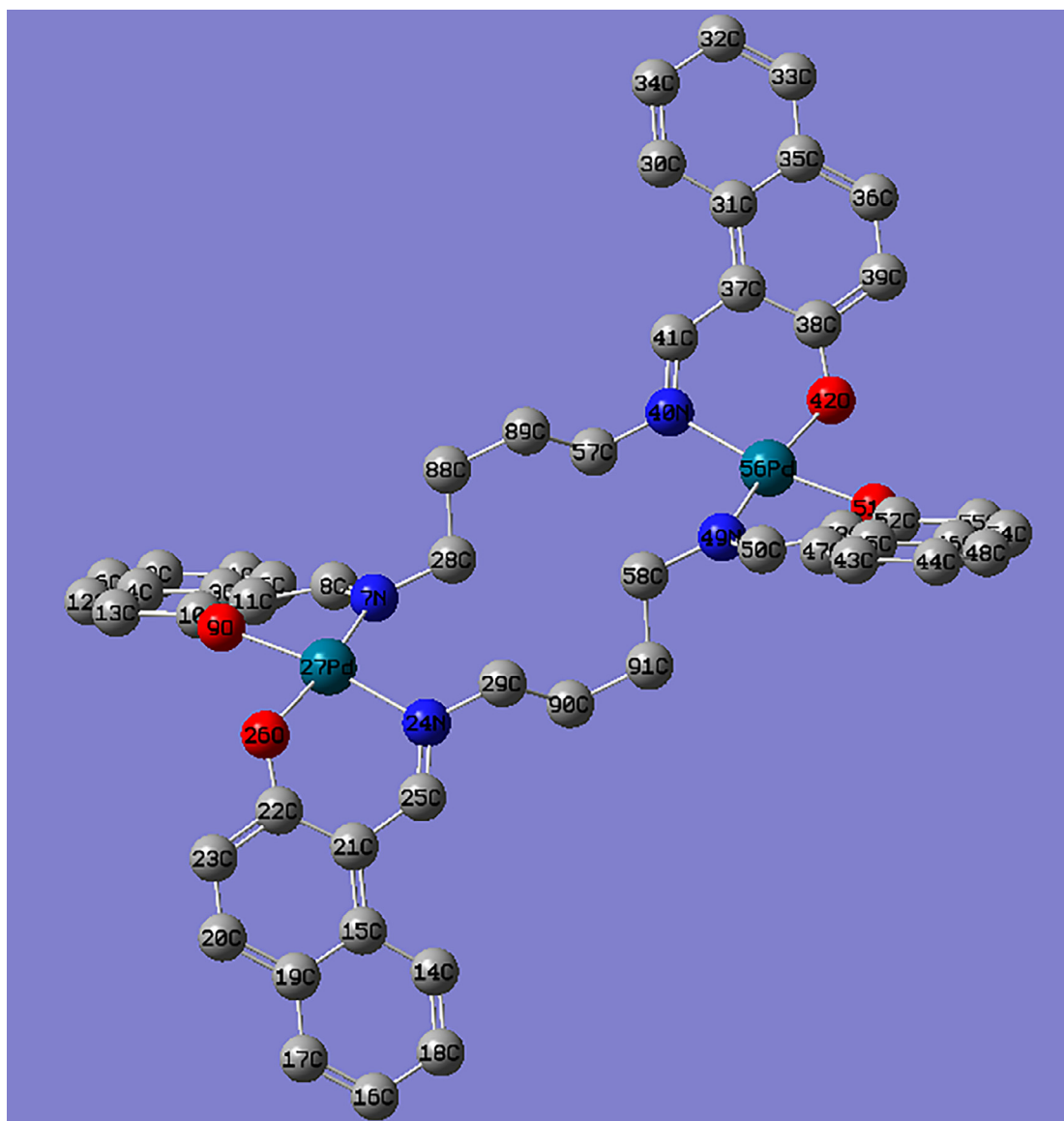


Fig. 7. The optimized geometry of the diimine palladium(II) complex **3** based on DFT calculations, the dimer structure.

Table 12

Bond angles ($^{\circ}$) of palladium(II) complex **6**, (PdL_2^*) experimental and theoretical.

Experimental ($\tau_4 = 0.0027$)	Theoretical** ($\tau_4 = 0.0067$)	Δ		
O3 – Pd1 – O4	90.44	O3 – Pd1 – O4	90.4261	0.0139
O2 – Pd1 – O4	179.86	O2 – Pd1 – O4	179.5245	0.3355
O1 – Pd1 – O4	90.040	O1 – Pd1 – O4	90.04600	0.0060
O3 – Pd1 – O2	89.120	O3 – Pd1 – O2	89.1032	0.0168
O3 – Pd1 – O1	179.75	O3 – Pd1 – O1	179.5256	0.2244
O2 – Pd1 – O1	90.400	O2 – Pd1 – O1	90.4247	0.0247

*L is 2-hydroxy-1-naphthaldehyde; **Values determined from DFT calculations (see section 3.7.). The labeling of the atoms in the third column can be related to those of S28 as follows: O1, O2, O3 and O4 correspond to O19, O41, O40 and O39 respectively.

Table 13

Bond lengths (\AA) of palladium(II) complex **6**, (PdL_2^*) experimental and theoretical.

Experimental	Theoretical**	Δ		
O4 – Pd1	1.959533	O4 – Pd1	2.0236	0.0641
O3 – Pd1	1.997629	O3 – Pd1	2.0110	0.0134
O2 – Pd1	1.993967	O2 – Pd1	2.0109	0.0170
O1 – Pd1	1.958379	O1 – Pd1	2.0237	0.0654

*L is 2-hydroxy-1-naphthaldehyde; **Values determined from DFT calculations (see section 3.7.). The labeling of the atoms in the third column can be related to those of S28 as follows: O1, O2, O3 and O4 correspond to O19, O41, O40 and O39 respectively.

3.8. Catalytic hydrogenation of cyclohexene

Hydrogenation of the unsaturated bonds by molecular hydrogen involves a flow of electrons from the highest occupied molecular orbital (HOMO) of one reaction partner to the lowest unoccupied molecular orbital (LUMO) of the other. Electron movement

between orbitals cannot occur unless the orbitals meet the symmetry requirement. For a bimolecular reaction, $\text{H}_2 + \text{C}=\text{C}$, the requirement is simply, that the two orbitals should have a net overlap.

For the current case, the direct reaction between $\text{C}=\text{C}$ of cyclohexene and H_2 could be achieved either by the interaction of the molecular orbital LUMO of H_2 (σ^*) with the corresponding molec-

Table 14
Bond angles (°) of palladium(II) complex **3**, (PdL³).

Pd27; ($\tau_4 = 0.1476$)		Pd56; ($\tau_4 = 0.1476$)	
N7 - Pd27 - O9	86.4515	N40 - Pd56 - O42	85.497
N7 - Pd27 - N24	103.5371	N40 - Pd56 - N49	103.539
N7 - Pd27 - O26	169.6727	N40 - Pd56 - O51	169.6616
O9 - Pd27 - N24	169.6583	O42 - Pd56 - N49	169.6734
O9 - Pd27 - O26	84.3238	O42 - Pd56 - O51	84.3279
N24 - Pd27 - O26	85.4969	N49 - Pd56 - O51	86.4455

Table 15
Bond lengths (Å) of palladium(II) complex **3** (PdL³).

Pd27		Pd56	
N7 - Pd27	2.0755	N40 - Pd56	2.0927
O9 - Pd27	2.0269	O42 - Pd56	2.0314
N24 - Pd27	2.0927	N49 - Pd56	2.0755
O26 - Pd27	2.0315	O51 - Pd56	2.0269

ular orbital HOMO of the C=C (π); in this case electrons flow from π orbital of C=C to σ^* of H₂. On the other hand, molecular orbital interaction can occur between the LUMO of C=C (π^*) with the HOMO of H₂ (σ) and here the electrons flow from σ orbital of H₂ to π^* of C=C. But neither the molecular orbitals σ of H₂ and π^* of C=C nor π of C=C and σ^* of H₂ have not any net overlap, hence the reaction is "symmetry forbidden".

Generally, the role of the present palladium(II) Schiff base complexes (catalysts) is to circumvent these symmetry restrictions. The catalytic role played by the metal center is likely due to the formation of an olefin metal bond in one of two ways. The first way includes bond formation via the back donation from filled d-orbital to the empty molecular orbital LUMO (π^*) of the olefin. The transferring of the electron density to the LUMO orbital, π^* , of the olefin, will lead to that this orbital becomes now, partially, a HOMO; obviously has the correct symmetry to interact with the LUMO orbital σ^* of H₂ molecule. The second route may pass through the flow of electrons from the olefin bonding orbit π to an empty orbital of the metal. The loss of the electron density of π orbital of olefin in the metal - olefin σ bond makes this orbital (π), in part a LUMO, has the suitable symmetry to accept the electrons flow from the HOMO σ orbit of H₂.

One may express these effects of the transition metal center are due to the exchange of electrons with incorrect symmetries across its orbital system to change them into right symmetries.

As a part of this work, the existing palladium(II) complexes were employed as catalysts for cyclohexene hydrogenation by H₂. Initial ratings for the palladium(II) complexes in the cyclohexene hydrogenation were carried out at hydrogen pressure of 490 mm Hg, 22°C, catalyst and cyclohexene concentrations are 0.0026 and 0.04 M respectively. Under these conditions, the current complexes showed catalytic activities to afford 100% cyclohexane with conversions ranging from 80.34% to 99% within 150 h. In order to confirm the catalytic potential of the examined palladium(II) complexes in fully observed catalytic hydrogenation reactions, blank experiments were performed without using the catalysts under the prevailing experimental conditions. The absence of cyclohexane formation in these blank trials confirmed the catalytic tendency of palladium(II) complexes in question. The catalytic activity of hydrogenation catalysts candidates is represented in two terms using the relations:

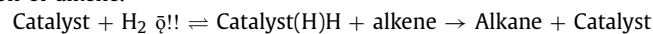
$$\text{Yield percentage} = [\text{product} / (\text{reactants} + \text{product})] \times 100$$

The catalytic activity was studied in relation to the effect of catalyst structure, catalysis type, nature and amount of the solvents and co-solvents.

3.8.1. Effect of the catalysis type

Under prevailing catalytic experimental conditions and with exception of [PdL²] in DMF, it is difficult to achieve a specific catalysis type since in other solvents used a certain amount of the catalysts is always soluble. However, the yield percentage (Table 16) remains fairly constant indicating that the candidate palladium(II) complexes can catalyze the hydrogenation of cyclohexene by both homogeneous and heterogeneous catalysis. It is assumed that during the catalytic hydrogenation cycle of alkene by a transition metal, both H₂ and olefin must exist together in the coordination sphere of the transition metal center to achieve effective hydrogenation. Regarding the precedence for entry of reaction partners in the coordination sphere of the transition metal center, there are two possibilities namely the hydride route and the olefin route.

The hydride route includes activation of H₂ on the metal center as a primary step, with subsequent coordination and hydrogenation of alkene.



In the olefin route, the olefinic substrate molecule first coordinatively bonded to the catalyst



For the hydride route, approaching H₂ to the square planar palladium(II) center must proceed in the Z-direction since the equatorial xy-plane is occupied by the diimine ligand molecule. In this situation the 4d_{z²} orbital must be lifted energetically and the change in the energy state of this orbital is reached through the addition of a suitable electron donor in the axial position, and the addition could proceed through the 5p_z orbital, which acts as an electron acceptor. The alkene coordination with palladium(II) occurs without barriers in the similarity to a reported case where the stabilizing energy resulting from this coordination was calculated to be 35.1 kJ/mol [28]. Therefore the initiation step is coordination of cyclohexene to the palladium(II) center to lift the doubly occupied 4d_{z²} orbital. Consequently, the five coordinated cyclohexene palladium(II) complex is the key intermediate in the catalytic cycle. The orbital interaction between the palladium(II) center and the H₂ molecule can be explained by the proper geometrical interaction of the energetically lifted 4d_{z²} orbital with the LUMO of the H₂ molecule, which can be achieved by the "end on" overlapping of both orbitals, σ^* (LUMO) of H₂ and 4d_{z²} of palladium(II) center.

This discussion explains that the running diimine palladium(II) complexes, whether completely or partially insoluble, are pre-catalysts that acquire their catalytic effectiveness in the reaction medium by binding to cyclohexene.

3.8.2. Effect of the catalyst structure

The values of cyclohexane yield (Table 16) demonstrate that, the alkyl bridge length between the two azomethine nitrogens has no effect on the catalytic activity of studied palladium(II) complexes. This can be attributed to the fact that all the examined palladium(II) complexes have the same square planar geometry. Since the Schiff base ligand molecule in these complexes is in the xy plane, the atoms within the bridge are not too far off this plan. This means that they do not present any substantial steric hindrance for the coordination of the central metal ion with the hydrogen molecule or with cyclohexene. This is also in a good agreement with the above discussion in which it is supposed that the catalytic role of the current palladium(II) complexes is mainly achieved through the interaction of the energetically lifted 4d_{z²} orbital (HOMO) of the metal with the LUMO of the H₂ molecule.

In the same context, quantitative comparison of the hydrogenation of cyclohexene using three naphthalendiimine palladium(II) complexes is represented in Fig. 8. It can be seen that there is a slight difference in the catalytic activity of the three represented complexes over a period of time 150 hours. Fig. 8 shows also, that the current catalytic hydrogenation reactions are kinetically very

Table 16
Yield % of cyclohexane in presence of palladium(II) or nickel(II) complexes.

Solvent	Yield %					
	PdL ¹ (NiL ¹)	PdL ² (NiL ²)	PdL ³ (NiL ³)	PdL ⁴ (NiL ⁴)	PdL ⁵ (NiL ⁵)	PdL ^{2*}
50 ml DMF	85.63	88.09	81.70	81.75	82.50	80.34
80 ml DMF	(6.76)	(69.19)	(9.31)	(3.42)	(6.39)	82.89
80 ml EtOH	90.51	92.75	85.42	84.62	89.89	84.65
DMF/EtOH	(6.10)	(6.75)	(8.38)	(6.75)	(5.31)	87.89
50 ml/30 ml	89.04	94.28	87.22	89.92	87.78	76.74
DMF/H ₂ O	(1.79)	(10.38)	(7.52)	(2.06)	(2.80)	76.42
	92.42	96.59	93.40	94.40	92.68	
50 ml/30 ml	(11.39)	(6.85)	(3.79)	(3.19)	(6.39)	
EtOH/H ₂ O	80.39	89.59	79.06	79.06	84.54	
50 ml/30 ml	(42.49)	(56.69)	(53.39)	(30.18)	(66.30)	
	88.39	92.75	90.40	91.40	92.00	
	(17.14)	(27.31)	(16.67)	(30.73)	(11.22)	

The values in parentheses are related to nickel(II) complexes of the current diimine ligands as reported in reference 8; *L is 2-hydroxy-1-naphthaldehyde

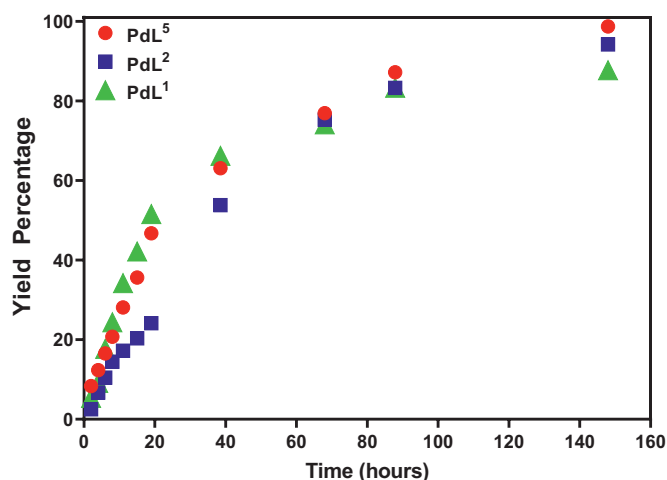


Fig. 8. Catalytic hydrogenation of cyclohexene by palladium(II) complexes.

slow in comparison to other transition metal complexes such as Wilkinson's catalyst [RhCl₂(PPh₃)₃] in which hydrogenation of cyclohexene was completely achieved within a few minutes [29]. The data in Table 16 display that the alkyl bridge length has no influence on the hydrogenation yield for complexes of both palladium(II) and nickel(II) with the present diimine ligands.

3.8.3. Solvent effects

Early studies have shown that the nature and quantity of the solvent and the co-solvent have a significant effect on the conversion of alkene to alkane by H₂ in catalytic hydrogenation reactions in presence of metal complexes [8,11,21]. DMF was the major solvent during current catalytic hydrogenation measurements because it is widely used for these types of reactions [30]. Additionally, it is assumed to be an important parameter in some catalytic hydrogenation pathways [30]. The different types and quantities of solvents and co-solvents used during the catalytic hydrogenation of cyclohexene by H₂ using the running diimine palladium(II) complexes are given in Table 17.

Table 16 shows that diimine palladium(II) complexes with high efficiency catalyze the hydrogenation of cyclohexene by H₂. Additionally, the data in Table 16 indicate that palladium(II) complexes are much more active than the analogous nickel(II) complexes where the yields of hydrogenation values are more than 10 times higher. It can be seen that on this higher level, the volume of the solvent and the composition of the solvent mixture slightly enhance the efficiency of the catalytic process.

Table 17
Solubility of H₂ in different solvents and co-solvents.

Solvent	Amount of dissolved H ₂ (cm ³)
50 ml DMF	1.26
80 ml DMF	2.02
80 ml EtOH	3.97
80 ml H ₂ O	0.94
50 ml DMF + 30 ml EtOH	1.61
50 ml DMF + 30 ml H ₂ O	2.75

These values are taken from reference [8]

It is noted that the use of ethanol alone or as a co-solvent improves the production of cyclohexane. This perhaps due to increase the solubility of hydrogen in ethanol compared to other solvents used as indicated in the table 16. On the other hand, addition of water as co-solvent in the case of nickel(II) complexes greatly enhances the production of cyclohexane up to 10 times. Vice versa occurs in the case of palladium(II) complexes, which indicates the difference in the mechanism of the hydrogenation reaction for these two types of metal complexes. This finding confirms the proposed olefin route for the catalytic role of the present palladium(II) catalysts and excluded the hydride route which depends to a large extent on the polarity of the reaction medium. In the same regard, it seems even that the most effective mixture (DMF/H₂O) found for the nickel complexes, gives a slight decrease with palladium complexes, but the differences are so small, that they are in the area of the accuracies of measurements. Under similar reaction conditions, the same drastic superiority of the catalytic activity of salicyaldiimine palladium(II) complexes was compared with the analogous nickel(II) complexes in the catalytic hydrogenation of 1-hexene [11].

3.8.4. Reaction mechanism

Since the current palladium(II) complexes are square planar, they cannot activate neither the substrate nor H₂ due to symmetry restrictions. The results in Table 16 support independence of the catalytic activity of palladium(II) complexes on the coordinating capability of the solvents used. Therefore the induction step is coordination of cyclohexene to the palladium(II) center to lift the doubly occupied 4d_{z²} orbital. Consequently, the current palladium(II) complexes are pre-catalysts and gain their catalytic potential during the catalytic hydrogenation process.

Based on these facts, the catalytic hydrogenation mechanism of cyclohexene is working across the olefinic pathway. In this case, the sequence of relevant steps should be as follows: i) Binding of alkene to the central palladium(II) ion.

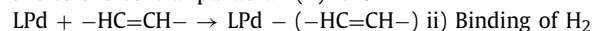
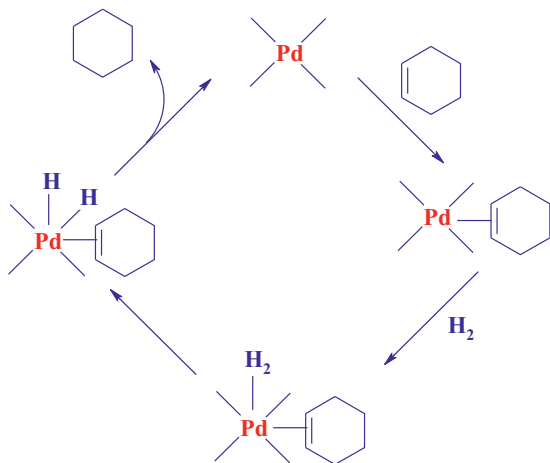


Table 18
Global reactivity descriptors of palladium(II) complexes and cyclohexene percentage.

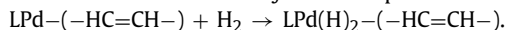
Compound	E _{LUMO} (eV)	E _{HOMO} (eV)	ΔE(eV)	μ	η	ω	*Yield %
PdL ¹	-1.90810	-5.22710	3.319048	-3.56762	1.659524	3.834829	92.42
PdL ²	-1.87899	-5.21219	3.333190	-3.54558	1.666599	3.771511	96.59
PdL ³	-1.91518	-5.20647	3.291290	-3.56080	1.645640	3.852430	93.40
PdL ₂	-2.45724	-5.85140	3.394153	-4.15430	1.697076	5.084737	87.89
Cyclohexene	1.17038	-6.25114	7.42152	3.71076	-2.54038	0.869570	-

*The catalytic hydrogenation reactions were carried out in a mixture of DMF (50 ml) and EtOH (30 ml);
T = 22°C; P = 490 mm Hg H₂; time = 150 h

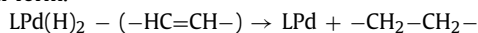


Scheme 2. Catalytic hydrogenation cycle of cyclohexene by palladium(II) complexes.

Binding of H₂ to palladium(II) center via oxidative addition results in the formation of di-hydride complex.



After cyclohexene coordination, binding of H₂ to form LPd(H)₂(HC=CH) is strongly exothermic and thus thermodynamically favorable. Once this complex has been formed, both alkene insertion and subsequent reductive alkane elimination have low barriers. In order to facilitate the transferring of hydrides to the carbon atoms of the double bond, H₂ binding must be in the suitable *cis* position to the coordinated alkene in the formed intermediate, LPd(H)₂(-HC=CH-). At this stage, a one of the ligand arms in the equatorial plan can be opened to allow H₂ to be bonded in the *cis* position to cyclohexane. iii) In successive steps the two hydrogen atoms transfer from the palladium center to the carbon atoms of the double bond with the simultaneous dissociation of alkane (reductive elimination) and the catalyst returns to its original form.



The catalytic cycle which takes into account the relevant steps mentioned above is shown in [Scheme 2](#).

3.8.5. Theoretical insights of the hydrogenation reactions of cyclohexene

Because of the high efficiency and accuracy of the DFT technique, it is widely used to estimate a variety of molecular properties [31]. To further understand the catalyst structure influence on the hydrogenation efficiency of cyclohexene, DFT study was performed. Based on B3LYP/Lanl2DZ level, DFT calculations were used to determine the energy of the frontier molecular orbitals, E_{HOMO} and E_{LUMO}, and the relevant chemical reactivity parameters like the energy gap (ΔE), chemical hardness (η), electronic chemical potential (μ), and electrophilicity indicator (ω). The obtained results in the case of palladium(II) complexes **1**, **2**, **3** and **6** in addition to cyclohexene are summarized in [Table 18](#) along with the

catalytic activity of the studied metal chelates. The first concept from the data recorded in a [Table 18](#) is the observed stability of the palladium(II) complexes in question because the energy values of frontier molecular orbitals (E_{HOMO} and E_{LUMO}) are all negative. As we see in [Table 18](#) the alkyl bridge length between the two donors nitrogen atoms of the azomethine linkage has slight effect on the energies of the frontier molecular orbitals of the palladium(II) complexes in question. It is well known that the energies of both HOMO and LUMO are often used as indicators of a molecule's readiness to donate and accept electrons [32]. As well, the values of the energies of HOMO and LUMO for both cyclohexene and palladium(II) complexes indicate that the HOMO for cyclohexene is a good donor and the LUMO of palladium(II) complexes is a good acceptor of electrons [33]. This finding is consistent with the aforementioned that the catalytic hydrogenation mechanism of cyclohexene is working across the olefinic pathway and that the current palladium(II) complexes are pre-catalysts acquire their catalytic activity in the reaction medium by binding to the cyclohexene.

In a similar study, it was established that there was a relationship between the catalytic activity of palladium(II) complexes for alkene hydrogenation and HOMO-LUMO energy gaps (ΔE) that promote coordination of alkene to the palladium(II) center [34]. The data in [Table 18](#) indicate that the differences in ΔE values are slight and comparable with the slight differences in the catalytic activity of the palladium(II) chelates in question. Other promoters for the catalytic activity of the examined palladium(II) complexes are the global reactivity descriptors η, μ, and ω. The results in [Table 18](#) show slight differences in the determined values of these promoters of reactivity and stability in conformity with that reported for the correlation between ΔE values and trend in the catalytic activity. The results in [Table 18](#) show slight differences in the values specified for these promoters of activity and the stability of the metal chelates in line with those reported for the relationship between the values of ΔE and the trend in the catalytic activity.

In light of the above and considering that the palladium(II) complexes under study are similar in their molecular structural properties, this has been reflected on the energies of the HOMO and LUMO orbitals and consequently on their catalytic activity.

4. Conclusion

In the present work a new series of palladium(II) complexes with quadridentate bis ortho naphtholimine ligands derived from 2-hydroxy-1-naphthaldehyde were synthesized and fully described structurally. Two methods were used to prepare this series of palladium(II) chelates based on the length of the alkyl bridge between the donor sites of the diimine ligands ([Scheme 1](#)). Based on spectroscopic and computer studies, the overall molecular geometry of the palladium(II) ion is the square planar, as expected for the d⁸ metal centers. At room temperature and 490 mm Hg of H₂ pressure, the current palladium(II) complexes are effective pre-catalysts for the hydrogenation of the mono olefin cyclohexene. The catalytic activity was studied in relation to the effect of catalyst structure,

catalysis type, nature and amount of the solvents and co-solvents. The current palladium(II) complexes, whether fully or partially soluble, are pre-catalysts whose catalytic activity is acquired in the reaction medium by binding to cyclohexene. Consequently, the five coordinated cyclohexene palladium(II) complex is the key intermediate in the catalytic cycle. In the light of the obtained results, the catalytic hydrogenation mechanism of cyclohexene is working across the olefinic pathway. DFT calculation demonstrated that: as a result of the fact that the palladium(II) complexes under study have similar structural properties, this was reflected in the energies of the HOMO and LUMO orbitals and consequently on their catalytic activity.

Declaration of Competing Interest

The authors declare that there are no conflicts of interest regarding the publication of this research paper.

Deposition number: 689635 (<https://www.ccdc.cam.ac.uk/deposit/enhancedata>)

Acknowledgements

Taif University Researchers Supporting Project number (TURSP-2020/05), Taif University, Taif, Saudi Arabia.

Supplementary materials

Supplementary material associated with this article can be found, in the online version, at doi:10.1016/j.jorganchem.2021.121764.

References

- [1] J. Hartwig, in: *Organo transition Metal Chemistry: From Bonding to Catalysis*, University Science Books, Sausalito, California, 2010, p. 575.
- [2] a) M.L. Shilpa, V. Gayathri, *Transition Met Chem* 41 (2016) 393; b) Q. Zhao, D. Chen, Y. Li, G. Zhang, F. Zhang, X. Fan, *Nanoscale* 5 (2013) 882; c) R.P. Yu, J.M. Darmon, C. Milsman, G.W. Margulieux, S.C.E. Stieber, S. DeBeer, P.J. Chirik, *J Am. Chem. Soc.* 135 (35) (2013) 13168.
- [3] a) J. Barbier, E. Lamy-Pitara, P. Marecot, J.P. Boitiaux, J.P. Cosyns, F. Verna, *Adv. Catal.* 37 (1990) 279; b) L.V. Nosova, V.I. Zikovskii, Y.A. Ryndin, *React. Kinet. Catal. Lett.* 53 (1994) 131; c) L.-M. Tang, M.-Y. Huang, Y.-Y. Jiang, *Macromolecules* 15 (1994) 527; d) V.M. Frolov, *Platinum Metals Rev* 40 (1996) 8.
- [4] a) F.P. da Silva, J.L. Florio, L.M. Rossi, *ACS Omega*, 2 (2017) 6014; b) D. Schleyer, H.G. Niessen, J. Bargon, *New J. Chem.* (2001) 423; c) J. Navarro, M. Sagi, E. Sola, F.J. Lahoz, I.T. Dobrinovitch, A. Katho, F. Joo, L.A. Oro, *Adv. Synth. Catal.* 345 (2003) 280; d) F. Neroszi, *Platin. Met. Rev.* 56 (2012) 236; f) M. Irfan, T.N. Glasnov, C.O. Kappe, *Chem. Sus. Chem.* 4 (2011) 300.
- [5] E. Negishi, in: *Handbook of Organopalladium Chemistry for Organic Synthesis*, Wiley & Sons, New York, 1, 2002, p. 229.
- [6] G. Henrich-Olive, S. Olive, *J. Mol. Catal.* 1 (1976) 121.
- [7] a) Q. Knijnenburg, A.D. Horton, H. van der Heijden, T.M. Kooistra, D.G.H. Hettterscheid, J.M.M. Smits, B. de Bruin, *J. Mol. Catal. A: Chemical* 232 (2005) 151; b) B. De Bruin, E. Bill, E. Bothe, T. Weyhermuller, K. Wieghardt, *Inorg. Chem.* 39 (2000) 2936; c) P.H.M. Budzelaar, B. De Bruin, A.W. Gal, K. Wieghardt, J.H. Van Lenthe, *Inorg. Chem.* 40 (2001) 4649; d) H. Sugiyama, G. Aharonian, S. Gambarotta, G.P.A. Yap, P.H.M. Budzelaar, *J. Am. Chem. Soc.* 124 (2002) 12268; e) Q. Knijnenburg, D. Hettterscheid, T.M. Kooistra, P.H.M. Budzelaar, *Eur. J. Inorg. Chem.* 6 (2004) 1204; f) R.P. Yu, J.M. Darmon, C. Milsman, G.W. Margulieux, S.C.E. Stieber, S. DeBeer, P.J. Chirik, *J. Am. Chem. Soc.* 135 (35) (2013) 13168.
- [8] A.M. Ramadan, W. Sawodny, H.Y.F. El-Baradie, M. Gaber, *Transition Met. Chem.* 22 (1997) 211.
- [9] M.R. Fox, P.L. Orioli, E.C. Lingafelter, L. Sacconi, *Act Cryst.* 17 (1964) 1159.
- [10] A.M. Ramadan, S.Y. Shaban, M.M. Ibrahim, A.A.-H. Abdel-Rahman, S.A. Sallam, S.A. Al-Harbi, W. Omar, *New J. Chem.* 44 (2020) 6331.
- [11] R. Ohl, Dissertation, Ulm University, Germany, 1990.
- [12] K. Nakamoto, *Infrared and Raman Spectra of Inorganic and Coordination compounds*, Wiley, New York, 1986.
- [13] K. Yamanouchi, S. Yamada, *Inorg Chim Acta* 12 (1975) 9.
- [14] A.B.P. Lever, *Inorganic Electronic Spectroscopy*, 2nd Ed., Elsevier, Amsterdam, 1970.
- [15] S.I. Shupack, E. Billing, R.J.H. Clark, R. Williams, H.B. Gray, *J. Am. Chem. Soc.* 86 (1964) 4594.
- [16] a) A.M. Ramadan, T.I. El-Emary, *Transition Met. Chem.* 23 (1998) 491; b) A. Gorg, J.P. Tandon, *Synth. React. Inotg. Met-org Chem.* 18 (7) (1988) 705; c) D.S. Martin, M.M. Tucker, *Inorg. Chem.* 5 (1966) 1298.
- [17] K. Yamanouchi, S. Yamada, *Bull. Chem. Soc. Japan* 42 (1969) 2543 K. Dey, R. L. De, *Inorg. Chem.*, 37 (1975) 1530.
- [18] L. Yang, D.R. Powell, R.P. Houser, *Dalton Trans* (2007) 955.
- [19] L.M. Shkol Nikova, E.M. Yumal, E.A. Shugam, V.A. Voblikova, *J Struct. Chem. (USSR)* 11 (1970) 819.
- [20] K. Durrstein, M. Sc., Thesis, Ulm University Germany, 1991.
- [21] R. Ohl, M. Sc. Thesis, Ulm University Germany, 1988.
- [22] E. Frasson, C. Panttoni, *Acta Cryst.* 17 (1964) 85.
- [23] a) M.A. Mahmoud, A.M. Abbas, S.A. Zaitone, A.M. Ammar, S.A. Sallam, *J. Mol. Struct.* 1180 (2019) 861; b) W. I. F. David, K. Shankland, L. B. Mccusker, C. H. Baerlocher, *Structure Determination from Powder Diffraction Data*, Oxford University Press Inc.: New York, (2002); c) D.M. Oliveira, W.N. Muscel, L.P. Duarte, G.D.F. Silva, H.A. Duarte, E.C.L. Gomes, L. Guimarães, S.A.V. Filho, *Quim. Nova* 35 (10) (2012) 1916; d) C.E. Hughes, G.N.M. Reddy, S. Masiero, S.P. Brown, P.A. Williams, K.D.M. Harris, *Chem. Sci.* 8 (2017) 3971; e) A.M. Ramadan, S.Y. Shaban, M.M. Ibrahim, F.I. El-Shami, S.A. Al-Harbi, *J. Mol. Struct* 1189 (2019) 360; f) A.M. Ramadan, S.Y. Shaban, M.M. Ibrahim, S.A. Sallam, F.I. El-Shami, S. Al-Juaid, *J Mater Sci* 55 (2020) 6457.
- [24] A. Altomare, C. Cuocci, C. Giacovazzo, A. Moliterni, R. Rizzi, N. Corriero, A. Falicchio, *EXPO 2013: a kit of tools for phasing crystal structures from powder data*, *J. Appl. Cryst.* 46 (2013) 1231.
- [25] a) M.D. Hobday, T.D. Smith, *Coord. Chem. Rev.* 9 (1973) 311; b) F.S. Nworie, *J Anal Pharm. Res.* 3 (6) (2016) 76.
- [26] M. J. Frisch, G. W. Trucks, H. B. Schlegel, *Gaussian 09, Revision A. 02*, Gaussian, Inc., Wallingford 2009
- [27] A.D. Becke, *J. Chem. Phys.* 98 (1993) 5648 C. Lee, W. Yang, R. G. Parr, *Phys. Rev. B*, 37, (1988) 785; P. J. Stevens, F. J. Devlin, C. F. Chablowski, M. J. Frisch, *J. Phys. Chem.*, 98, (1994) 11623.
- [28] P.A. Chaloner, M.A. Esteruelas, F. Joo, L.A. Oro, in: *Homogeneous Hydrogenation*, Kluwer Academic Publishers, 1994, p. 5.
- [29] G.H. Olive, S. Olive, *Coordination and Catalysis, Monographs in Modern Chemistry, Volume 9*, Verlag Chemie, 1977.
- [30] a) F.R. Hartley, J.A. Davis, *Rev. Inorg. Chem.* 4 (1982) 27; b) A. Bose, C.R. Saha, *J. Mol. Catal.* 49 (1982) 271.
- [31] a) A. Suvitha, S. Periandy, S. Boomadevi, M. Govindarajan, *Spectrochim. Acta A* 117 (2014) 216–224; b) S. Ramalingam, S. Periandy, M. Govindarajan, S. Mohan, *Spectrochim. Acta A* 75 (2010) 1308.
- [32] V. Karunakaran, V. Balachandran, *Spectrochim. Acta A* 98 (2012) 229.
- [33] S. Sagdinc, B. Koksoy, F. Kandemirli, S.H. Bayari, *J. Mol. Struct.* 917 (2009) 63.
- [34] a) T. Sperger, I.A. Sanhueza, I. Kalvet, F. Schoenebeck, *Chem. Rev.* 115 (2015) 9532; b) T. A. Tshabalala and S. O. Ojwach, doi:10.20944/preprints201804.0364.v1.